DOE/NASA/20320-44
NASA TM-83309

Structural Qualification Testing and Operational Loading on a Fiberglass Rotor Blade for the Mod-0A Wind Turbine

Timothy L. Sullivan
National Aeronautics and Space Administration
Lewis Research Center

March 1983

Prepared for
U.S. DEPARTMENT OF ENERGY
Conservation and Renewable Energy
Wind Energy Technology Division

Printed in the United States of America

Available from
National Technical Information Service
U.S. Department of Commerce
5285 Port Royal Road
Springfield, VA 22161

NTIS price codes[1]
Printed copy: A02
Microfiche copy: A01

[1]Codes are used for pricing all publications. The code is determined by the number of pages in the publication. Information pertaining to the pricing codes can be found in the current issues of the following publications, which are generally available in most libraries: *Energy Research Abstracts (ERA); Government Reports Announcements* and Index (*GRA* and I); *Scientific and Technical Abstract Reports (STAR);* and publication, NTIS-PR-360 available from NTIS at the above address.

DOE/NASA/20320-44
NASA TM-83309

DOE/NASA/20320--44

DE83 011565

Structural Qualification Testing and Operational Loading on a Fiberglass Rotor Blade for the Mod-0A Wind Turbine

Timothy L. Sullivan
National Aeronautics and Space Administration
Lewis Research Center
Cleveland, Ohio 44135

March 1983

Prepared for
U.S. DEPARTMENT OF ENERGY
Conservation and Renewable Energy
Wind Energy Technology Division
Washington, D.C. 20545
Under Interagency Agreement DE-AI01-76ET20320

STRUCTURAL QUALIFICATION TESTING AND OPERATIONAL LOADING ON A FIBERGLASS ROTOR BLADE FOR THE MOD-0A WIND TURBINE

Timothy L. Sullivan

National Aeronautics and Space Administration
Lewis Research Center
Cleveland, Ohio 44135

SUMMARY

The original blades used in the 200-kW Mod-0A wind turbine program began to show signs of structural problems after less than 1000 hr of operation. These blades were made of aluminum with riveted construction typical of an airplane wing. In addition to having structural problems, these blades were very expensive and showed little potential for reduced cost in volume production. Therefore, a program was initiated to develop blades for Mod-0A service that were not only structurally adequate but that showed potential for low cost when produced in significant quantities (>100). As a part of this program a fiberglass blade was designed and two blades were fabricated using a tape winding process. During the design phase of this program, two areas of the blade were identified where structural testing in the laboratory would reduce the risk of problems in the field. The first area was the blade root retention where a transition between fiberglass and steel is made. Here the concern was debonding between steel and fiberglass under fatigue loading. The second area was the outboard portion of the main structural spar of the blade. Here the concern was buckling of the spar under the limit load condition. Therefore, these two areas were qualified by test. This report describes these tests and their results. In addition, a comparison is made of expected blade loading and loading measured in the field. Finally, the report documents results of measurements of natural frequency, damping ratio, and deflection under load made on the operational blades.

Fatigue testing was performed on two half-scale root retention specimens and on one full-size root end section. Fatigue loading was scheduled to first qualify the root end design by applying the high load end of the fatigue spectrum. When no failure occurred during this phase, a second phase was begun with the purpose of failing the part. The load cycling results showed that the root end significantly exceeded design requirements. The main structural spar was qualified by applying the design limit load to both operational blades before installation in the field. This proof test was conducted without incident. The fatigue and static tests showed that the fiberglass blades were qualified for operation on Mod-0A in continuous utility service.

The fiberglass blades were installed on the 200-kW Mod-0A wind turbine at Clayton, New Mexico, where they operated for nearly 1 yr and accumulated about 3000 hr of synchronous operation. Flatwise and chordwise blade loads were measured during this period. These loads showed good agreement with expected loading based on analysis and previous experience. The measured loads also showed the conservative nature of the loading used to qualify the root retention in fatigue. Testing both in the laboratory and in the field has given high confidence in the ability of the fiberglass blade to achieve its design life of 30 yr (4×10^8 cycles).

INTRODUCTION

Under the overall direction of the U.S. Department of Energy, the Federal Wind Energy Program is developing wind turbines that will convert wind energy to electrical energy in a cost-effective manner. As part of this program, the NASA Lewis Research Center is directing the development of large (>100 kW), horizontal-axis wind turbines. In early wind turbines developed in the Lewis program, such as the 200-kW Mod-0A (ref. 1), the cost of the rotor blades was a large percentage of the total wind turbine cost. The original Mod-0A blades were made of aluminum. Their construction was typical of that used to make an airplane wing with skins riveted to ribs and stringers. In addition to their high cost, structural problems in these blades (ref. 2) caused long down times in field operations. Therefore, it became a high priority to develop blade designs that were structurally reliable for Mod-0A service and that showed potential for low cost. Contracts were awarded to several organizations on a competitive basis.

One of these contracts was awarded to Structural Composites Industries (SCI) of Pomona (formerly of Azusa), California, to design and fabricate a set of transverse filament tape (TFT) fiberglass blades for service on the 200-kW Mod-0A wind turbine. Details of the design, analysis and fabrication of this blade were reported by Weingart (ref. 3). During the design phase of this contract, two areas of special concern were identified. The first was a concern about buckling of the main structural spar under the limit (hurricane) load. An earlier test of a spar fabricated using the same process resulted in a premature failure. This spar had been fabricated in a program to develop a 45.7-m (150-ft) long wind turbine blade. Details of this program were reported by Gewehr (ref. 4). The second area of concern was the reliability under cyclic loading of the root end where a transition from fiberglass to steel takes place. Transition areas had been a source of problems in earlier blades (ref. 2). Therefore, a program was initiated to qualify these critical areas of blade design by test.

The primary purpose of this report is to describe the qualification tests and document their results. During qualification testing of the spar, deflection under load and natural frequencies of the operational blades were measured. These measurements are compared with the results obtained from a finite element model used for analyses during the design phase of the program. In addition, the SCI fiberglass blade design will be described and structural design requirements listed. These blades operated on the Mod-0A wind turbine at Clayton, New Mexico, from August 1981 to June 1982 when the Mod-0A test program was completed. Measured blade load data will be discussed and compared with the loads used for design and in fatigue testing the root end.

DESIGN FEATURES AND STRUCTURAL REQUIREMENTS

Blade Design

The SCI fiberglass/epoxy blade was designed to operate on the Mod-0A wind turbine, a horizontal-axis machine rated at 200 kW (ref. 1). Its two-bladed rotor is 38.1 m (125 ft) in diameter and operates downwind of the tower. Rotor speed is 40 rpm. The hub is rigid with a precone angle of 7°, and is elevated 30.5 m (100 ft). Power control is achieved by full-span pitch of the blades. A photograph of a Mod-0A wind turbine is shown in figure 1.

The chord, thickness, and twist distributions for the blade are given in figure 2. The blade is fabricated using a tape winding process. The primary fiber material used is TFT. The transverse filaments are fiberglass held together with a warp material that is less than 1 percent of the total tape weight. A sample of TFT is shown in figure 3. Before winding, the TFT is impregnated with epoxy resin. The TFT is wound in the hoop direction so the fiberglass filaments are nearly parallel to the longitudinal axis of the blade. To provide adequate shear and transverse properties in the laminate, bias ($\pm 45^\circ$) filament tape (BFT) and longitudinal filament tape (LFT) are interleaved with the TFT. The tape winding process offered several advantages over a filament winding process. The most important are that (1) fiber material can be deposited at a very rapid rate, reducing fabrication time and, therefore, cost; (2) wall thickness can be tapered without the use of turnaround disks and the waste of material these disks require; and (3) TFT fibers can be alined in the direction requiring greatest strength and stiffness.

The blade cross section consists of three cells (fig. 4). The first two cells provide the required structure, and the third cell completes the airfoil shape. The first cell is wound on an extractable steel mandrel. The last two cells are wound on foam mandrels which remain in place. Initially, a two-cell design was considered (one structural cell). The three-cell design was selected because of its greater structural efficiency in resisting buckling loads. Its capability was proven by test. This will be described in a subsequent section.

The details of the blade root end where the material transitions from fiberglass to steel and where the bolt circle diameter is reduced to match the Mod-0A hub are shown in figures 5 and 6. The root end was designed to provide redundant retention of the blade. The primary retention is provided by the adhesive bond between the fiberglass and steel. Should that fail, mechanical retention is provided by the fiberglass that was wound into the recessed grooves of the steel fitting. This can be seen in the photograph of a half-scale root end section (fig. 5(b)). Through bolts are provided to prevent rotation between fiberglass and steel in the event of bond failure. Removal of the steel mandrel from the blade required a diameter larger than that which could mate directly with the Mod-0A hub. Therefore, a short conical adapter section was required to make the transition between the two diameters (fig. 6).

Structural Loads

The blade structural design was based on the requirement to meet two load conditions without material yielding or failure. The first load condition, a limit load condition, was a pressure of 2.8 kN/m^2 (50 lb/ft^2) applied flatwise to the blade plus the gravity load. This represented a load that might be seen in hurricane wind conditions. The spanwise bending moment distribution for this load is given in figure 7.

The second load case was a fatigue load condition. The MOSTAB-WTE computer program (ref. 5) was used to calculate blade loads for a wind speed of 18 m/s (40 mph), a rotor speed of 40 rpm, and a precone angle of 7°. These represent the cut-out wind speed, design rotor speed, and hub precone for the Mod-0A wind turbine. Calculated blade loads were then multiplied by contingency factors of 1.25 for cyclic flatwise bending and 1.10 for cyclic chordwise bending. These contingency factors were derived from previous operating experience with several Mod-0A wind turbines (ref. 6). With these load contingency factors, it was expected that the design values would represent the 99.9 percentile probability level. In other words, the design loads would be expected to be

exceeded only 0.1 percent of the time. To be conservative, the blade was designed to withstand these loads for 4×10^8 cycles, the number of rotor revolutions expected in the 30-yr design life. Spanwise distribution of the design fatigue loads is given in figure 8.

Based on (1) load cases specified by NASA, (2) blade cross-sectional properties, and (3) material allowable stresses, margins of safety were calculated for several stations along the blade span. Here, margin of safety (MS) is defined as

$$MS = \frac{\text{allowable stress}}{\text{applied stress}} - 1$$

These margins are plotted in figure 9 for both load cases. The figure shows that the inboard half of the blade is designed by fatigue with the margin becoming smallest at 10 percent of span where the transition from steel to fiberglass ends. The outboard half of the blade is designed by the limit load and the margin reaches a minimum at 70 percent of span. Therefore, to qualify this blade design for Mod-0A service, the inboard section was subjected to a fatigue test, and the outboard section to a proof test.

BLADE ROOT FATIGUE TESTING

Because the structural integrity of a rotor blade root end is important for safe and reliable wind turbine operation, the adequacy of the SCI design was verified by fatigue test. To reduce material and fabrication costs, half-scale specimens were designed for testing. Two specimens were fabricated. In the first, an attempt was made to match the full-size blade design in every important detail, including the bond between fiberglass and steel (bonded specimen). In the second, the bond between fiberglass and steel was intentionally eliminated by use of a mold release agent (unbonded specimen). This allowed the fatigue testing of the mechanical retention. In addition to the half-scale tests, a fatigue test was conducted on a full-size root end section that had been fabricated to check tooling and processing before the two full-length operational blades were manufactured. All fatigue testing was done with the ratio of minimum to maximum load approximately equal to zero ($R \approx 0$).

Half-Scale Tests

A sketch of the half-scale root end test specimen is shown in figure 10. The specimen included a half-scale conical adapter. The cross section was circular. Shear loads applied at the tip were controlled so that for a given loading condition the bending stress in the half-scale retention section matched that for the full-size blade. No attempt was made to match shear stresses. For the specimen geometry shown in figure 10, the shear stresses were about 15 percent greater than those in the full-size blade.

The bending stress in a beam can be calculated as follows: $\sigma = My/I$ where σ is the stress, M is the applied moment, y is the distance from the neutral axis, and I is the moment of inertia of the cross section. To match bending stresses in the full-scale and half-scale spars, the loads on the half-scale spar were one-eighth those for full scale, based on the following analysis:

$$\frac{M_s y_s}{I_s} = \frac{M_f y_f}{I_f} \qquad (1)$$

where the subscripts s and f refer to subscale and full-scale, respectively. For the half-scale case,

$$y_s = \frac{1}{2} y_f \tag{2}$$

and

$$I_s = \frac{1}{16} I_f \tag{3}$$

Therefore, $M_s = 1/8\ M_f$. The applied moments for both the half- and full-scale cases are tabulated in table I. Included in this table are the sequence of loading, the significance of each loading condition, and the number of load cycles applied to qualify the root end design. Following qualification, additional load cycles were applied to induce failure.

The half-scale specimens were tested at the U.S. Army Applied Research and Technology Laboratory at Ft. Eustis, Virginia. A description of this facility can be found in reference 7. The bonded specimen was cycled at a rate of 5 Hz. The initial rate for the unbonded specimen was the same. However, when heat buildup was detected in the retention area, the rate was decreased to 3 Hz. No heat was detectable at the lower cyclic rate.

After surviving the initial loading spectrum, the bonded specimen was rotated 90° about the pitch axis before additional load cycles were applied. This was done to preserve any damage to the bond by placing the high stressed area on the neutral axis. After rotation, additional load cycles were applied at the load levels shown in table I until failure occurred. The unbonded specimen was cycled in the same orientation throughout the entire test.

As table I shows, both specimens survived the qualification load cycles. In addition they both survived 10^6 cycles up to the hurricane load level. After more than 3×10^5 cycles at the hurricane load level, failure occurred in the steel root end fitting of both specimens. The location of the failure is shown in figure 5.

After completion of load cycling, the root ends of both specimens were inspected. After visual and tap testing revealed no damage, the root ends were sectioned. Sectioning of the bonded specimen showed that the bond was totally intact. Visual inspection of the unbonded specimen showed that the fiberglass, including that in contact with the steel, was free from any apparent damage.

Full-Scale Test

The test of the full-scale root end section took place at the Structural Test Laboratory of NASA Johnson Space Center (JSC), Houston, Texas. Figure 11 is a photograph of the test setup. The blade section was 5.3 m (17.5 ft) long. The applied moments and number of cycles are given in table I. The cyclic rate was 1 Hz. As was the case with the half-scale specimens, no attempt was made to simulate the root end shear stress these blades would see in service. The shear load required to produce the desired root end bending moment produced a root end shear stress about 70 percent greater than that expected in actual service.

As table I shows, this blade section successfully withstood the design qualification load cycles. During the next stage of testing (to induce failure), failure occurred in several bolts that attached the conical adapter to the JSC structural support (strongback). This failure occurred after more

than 300 000 cycles at the emergency shutdown load level in fasteners that are not a part of the Mod-0A blade design. Because little would be learned from additional load cycling and because the JSC facility was needed for other wind turbine blade tests, testing was terminated.

Comparison with Expected Load Spectrum

The test load spectrum, used to qualify the SCI blade root design and then to induce failure, can be compared with the load spectrum expected during operation (fig. 12). Load levels B, C, and D of the operational spectrum were based on experience obtained with other Mod-0A blades. Level E is the calculated hurricane load, and level A is the load calculated using MOSTAB with a wind speed that produces about half the rated power. The two load cases used to design the SCI fiberglass blades are also plotted in figure 12 to show their relationship to the expected operational and test load spectra.

The half- and full-scale tests showed that the SCI fiberglass blade not only met expected requirements for fatigue but substantially exceeded them.

STATIC TESTING

Static tests were performed on both operational blades (designated SN0018 and SN0019) before their installation on the Mod-0A wind turbine at Clayton. The blades were tested statically to verify that they could withstand the design limit load without buckling (i.e., a proof test). While the blades were attached to the wind turbine blade strongback at NASA Lewis for the proof tests, additional measurements were made. These measurements included deflection under load, natural frequency, and damping ratio. The deflection and natural frequency measurements provided a basis for checking the accuracy of a finite element model of the blade developed for this program. This model was used to determine natural frequency placement and to provide the modal representation of the blade required by the MOSTAB computer program.

Proof Test

Figure 13 shows the setup for the proof test and a photograph of a blade under load. Both blades withstood the design limit load without buckling and without any sign of distress. Both blades were tested so that a processing defect that might have occurred in one blade but not the other would be detected. Figure 14 compares the design limit load with the load applied during the proof test. The calculated minimum margin of safety against buckling occurred between 60 and 77 percent of span. No attempt was made to proof test inboard of 35 percent of span. The calculated margins of safety were large in this span, and there was concern about damaging the blade because of the high concentrated loads required to produce the desired bending moment. The successful passing of the proof test completed the qualification testing required for these blades.

Deflection under load was measured in the flatwise direction for both blades during the proof test and in the chordwise direction for one blade. In figure 15 these deflections normalized by the applied load are compared with calculations made using a finite element model of the blade cantilevered off a rigid support. The deflection due to rotation of the strongback has been subtracted from the measured values. The measured and calculated values agree quite closely. The data show that the actual stiffness of the blade was

slightly less than that used in the model. The flatwise measured data show a stiffness difference of about 5 percent between the two blades.

Natural Frequency and Damping

Measured and calculated natural frequencies are compared in table II. The data show a slight difference in natural frequency between the two blades. This difference is not considered significant when the accuracy of the measurement system is considered. The accuracy is estimated to be ±0.1 Hz. However, the trend of the measured data is consistent with the deflection under load data that showed SN0018 to be slightly stiffer than SN0019. The calculated values were obtained using the same finite element model of the blade used for deflection calculations. As figure 15 shows, the stiffness used in the model was slightly greater than the stiffness of the real blades. In addition the model had about 8 percent more mass than the real blades. These two factors would tend to compensate for each other when the model is used to calculate natural frequencies. Both a rigid end fixity and one estimated to match the flexibility of the strongback were modeled. Calculated natural frequencies using finite element methods can be expected to be within 5 percent of actual values. Table II lists the ratio of average-measured to calculated natural frequency. All the values are within the expected error range except for the first chordwise mode when the flexible retention model was used. The larger difference here indicates that this model, which considered the stiffness of the strongback but not its mass, may in certain cases exaggerate the decrease in natural frequency due to strongback flexibility. Considering all the results, the finite element model was a good representation of the operational blades.

Table II also includes flatwise and edgewise damping ratios measured on one blade. Damping values were obtained by exciting the blade by hand and recording the time history of the decaying output of a strain gage bridge mounted on the conical adapter of the blade. The log decrement method was used to calculate the damping ratio. The flatwise measurement may be a combination of structural and aerodynamic damping. Little aerodynamic damping would be expected in the edgewise direction. Therefore, the edgewise measurement is a more accurate indication of the structural damping in the blade. Because the measured values are so small, it can be concluded that structural damping is of little practical importance in the dynamic response of the operating SCI fiberglass blades.

OPERATIONAL DATA

The SCI fiberglass blades were installed on the 200-kW Mod-0A wind turbine at Clayton on August 19, 1981, and operated in continuous utility service until June 30, 1982, when the Mod-0A experimental test program was ended. During this period over 3000 hr of synchronous operation took place and nearly 300 MWh of energy were generated. The conical adapter of each blade was instrumented with strain gage bridges for measuring flatwise and chordwise bending moments at 5 percent of span. These bridges were calibrated during the static testing of the blades. In this section blade load data obtained during operation will be reviewed and compared with expected loads.

Transient Loads

Measured blade loads during several types of shutdowns are tabulated in table III. The data show that the magnitude of shutdown loads is more strongly affected by the wind speed than by the blade pitch rate. Normal shutdowns in high winds produce 66 percent more load than in low winds. When operating at about the same wind speed (4.5 to 5.5 m/s (10 to 12 mph)), the rapid shutdown produced 23 percent more load than the normal shutdown. These loads are compared with expected loading in figure 16. In all cases the measured loads were less than expected.

Fatigue Loads

The Mod-0A at Clayton operates in basically two types of atmospheric conditions: stable and unstable. Stable conditions normally occur at night and are characterized by low turbulence and high wind shear (wind shear exponent, α, of about 0.4). Unstable conditions usually occur during the day and are characterized by a lower wind shear ($\alpha \approx 0.1$) and greater turbulence. The wind speed associated with stable conditions is generally lower than that associated with unstable conditions. The spectrum of flatwise fatigue loads is strongly influenced by which of these two conditions exists. A third condition associated with surface roughness has been identified at the Clayton site. The wind turbine is located at the southern edge of Clayton, a town of about 3000 people. Occasionally the winds blow from the north and pass over the town before reaching the wind turbine. This condition is characterized by both high wind shear and high turbulence and results in increased cyclic flatwise blade loads.

Four cyclic flatwise blade load spectra that were obtained during operation at the Clayton site are presented in figure 17(a). Three of the spectra resulted from normal operation, and the fourth resulted from operation with large yaw error when the winds were from the north. Each spectrum represents 6 hr of operation. Comparison of case 1 with case 2 shows that stable conditions result in a much flatter distribution than do unstable conditions, but this flatter distribution has a significantly higher median level. Comparison of case 1 with case 3, two daytime spectra, shows how the cyclic flatwise loads respond to increasing wind speed. Case 4 is a spectrum produced when the winds were from the north. Because of a temporary misalinement of the wind direction sensor on the wind turbine, the machine was operating at the time with a yaw error of about 40°. Analysis of this yaw condition using MOSTAB showed that at the median (50 percentile) level about 19 kN-m (14 000 lb-ft) of flatwise cyclic load was due to yaw error. The remaining increase over loads previously observed (case 3) is attributed to higher wind shear and turbulence due to the wind passing over the town. This spectrum is the only one studied where the 0.999 probability level exceeds the design level. The SCI blades were not designed to sustain the case 4 level of loading for 30 yr.

A spectrum more representative of what these blades would be subjected to over their design life at the Clayton site was obtained by combining individual spectra selected at random. A combined spectrum is also shown in figure 17(a). This spectrum represents over 60 hr of operation (162 000 rotor revolutions) and includes the individual spectra shown in the figure. The average power for the combined spectra is about 130 kW; the average for all 3000 hr of operation is about 100 kW. Therefore, the actual spectrum of flatwise cyclic loads these blades have experienced during 3000 hr is probably slightly less than that represented by the combined spectrum.

Cyclic chordwise loads are dominated by gravity, and their spectra, therefore, are relatively flat. Higher odd harmonics, due primarily to hub motion, add to or subtract from the gravity moment. Chordwise spectra for three of the four conditions previously discussed are presented in figure 17(b). The 0.999 probability load level did not exceed the design level for these or any other spectra that were examined. A combined chordwise spectrum is shown in figure 17(b); it represents 87 000 rotor revolutions.

Spera and Janetzke (ref. 6) present cyclic blade load spectra for several other Mod-0A wind turbine configurations. In table IV spectra obtained from operation of the SCI fiberglass blades are compared with spectra obtained from operation of the Clayton Mod-0A with aluminum blades and from operation of a Mod-0A at Kahuku, Hawaii, with wood blades. The table shows that there was no significant difference among the cyclic blade load spectra of these three test configurations.

A resultant peak load spectrum (fig. 18) was developed using the combined measured-cyclic-load spectra of figure 17 and calculated values of steady load. These data were extrapolated to 4×10^8 cycles and are compared to the expected spectrum in the figure. The expected spectrum is a reasonable representation of the extrapolated measured data.

From this review of blade load data, it is concluded that the measured cyclic loads are consistent with expected loading and with the loads used to design the blades. The design life of 4×10^8 cycles should be achieved.

CONCLUSIONS

Structural qualification tests on the SCI fiberglass blades showed that all structural requirements were met. Fatigue tests of blade root end sections showed that fatigue requirements were substantially exceeded. Proof tests of two Mod-0A operational blades showed that design limit load requirements were met.

Approximately 3000 hr of operating experience were attained with the fiberglass blades. Representative measured blade loads showed that the spectrum of loads was close to that expected, giving high confidence that the 30-yr (4×10^8 cycle) design life can be achieved.

Measurement of deflection under load and natural frequencies of the two operational blades showed that the finite element model used for analysis was a good representation of the real blades.

REFERENCES

1. Andersen, T. S.; et al.: Mod-0A 200-kW Wind Turbine Generator Design and Analysis Report. (AESD-TME-3052, Westinghouse Electric Corp.; NASA Contract DEN3-163.) NASA CR-165128, 1980.

2. Linscott, B. S.; and Shaltens, R. K.: Blade Design and Operating Experience on the Mod-0A 200-kW Wind Turbine at Clayton, New Mexico. Large Wind Turbine Design Characteristics and R&D Requirements. NASA CP-2106, 1979, pp. 225-238.

3. Weingart, O.: Design, Evaluation and Fabrication of Low-Cost Composite Blades for Intermediate-Size Wind Turbines. (SCI-81520, Structural Composites Industries, Inc.; NASA Contract DEN3-100.) NASA CR-165342, 1981.

4. Gewehr, H. W.: Design, Fabrication, Test and Evaluation of a Prototype 150-Foot Long Composite Wind Turbine Blade. (CR-1575, Kaman Aerospace Corp.; NASA Contract NAS3-20600.) NASA CR-159775, 1979.

5. Spera, D. A.: Comparison of Computer Codes for Calculating Dynamic Loads in Wind Turbines. NASA TM-73773, 1977.

6. Spera, D. A.; and Janetzke, D. C.: Performance and Load Data from Mod-0A and Mod-1 Wind Turbine Generators. Proceedings of a Workshop on Large Horizontal-Axis Wind Turbines. R. W. Thresher, ed., NASA CP-2230, 1982, pp. 447-468.

7. Faddoul, J. R.; and Sullivan, T. L.: Structural Fatigue Test Results for Large Wind Turbine Blade Sections. Proceedings of a Workshop on Large Horizontal-Axis Wind Turbines. R. W. Thresher, ed., NASA CP-2230, 1982, pp. 303-328.

TABLE I. - SCI FIBERGLASS BLADE ROOT END FATIGUE TEST RESULTS

Load sequence	Significance of load	Peak applied moment, kN-m (lb-ft)		Number of cycles			
				Half scale			Full scale
		Half scale	Full scale	Bonded		Unbonded	
				Original orientation	Rotated 90°		
Phase 1: qualify design							
1	Design	25.8 (19.0×10^3)	207 (152×10^3)	1×10^6	-	1×10^6	1×10^6
2	High wind	29.9 (22.0×10^3)	239 (176×10^3)	1×10^6	-	1×10^6	1×10^6
3	Normal shutdown	33.3 (24.5×10^3)	267 (196×10^3)	2×10^5	-	2×10^5	2×10^5
4	Emergency shutdown	38.8 (28.5×10^3)	310 (228×10^3)	2×10^4	-	2×10^4	2×10^4
5	Hurricane	57.1 (42.0×10^3)	457 (336×10^3)	1×10^2	-	1×10^2	1×10^2
Phase 2: induce failure							
6	Normal shutdown	33.3 (24.5×10^3)	267 (196×10^3)	-	8.0×10^5	8.0×10^5	8.0×10^5
7	Emergency shutdown	38.8 (28.5×10^3)	310 (228×10^3)	-	9.8×10^5	9.8×10^5	[a] 3.1×10^5
8	Hurricane	57.1 (42.0×10^3)	457 (336×10^3)	-	[b] 3.6×10^5	[b] 3.8×10^5	-

[a] Attachment bolts failed; test terminated.
[b] Specimen failed in steel root end fitting.

TABLE II. - NATURAL FREQUENCIES AND DAMPING RATIOS FOR SCI FIBERGLASS BLADES

Mode	Measured frequency, Hz		Calculated frequency, Hz		Ratio of average measured to calculated frequency		Fraction of critical damping
	SN0018	SN0019	Rigid retention	Flexible retention[a]	Rigid retention	Flexible retention[a]	
First flapwise	1.6	1.5	1.51	1.47	1.03	1.05	0.008
First chordwise	2.9	2.8	2.89	2.57	.99	1.11	.003
Second flapwise	4.4	4.3	4.44	4.22	.98	1.03	---

[a]Stiffness, 81 600 kN-m/rad ($6x10^7$ lb-ft/rad).

TABLE III. - LOADS DURING SHUTDOWN OF SCI FIBERGLASS BLADES

[5 Percent span.]

Type of shutdown	Pitch rate, deg/sec	Wind speed, m/s (mph)	Peak load, kN-m (lb-ft)			Ratio of resultant to expected load
			Flatwise	Chordwise	Resultant	
Normal	[a]0.8	4.5 (10)	136 (100×10^3)	72 (53×10^3)	154 (113×10^3)	0.57
Normal	[a].8	17.8 (40)	245 (180×10^3)	75 (55×10^3)	256 (188×10^3)	.95
Rapid	3.2	5.4 (12)	158 (116×10^3)	105 (77×10^3)	189 (139×10^3)	.61
Safety system	.8	6.7 (15)	218 (160×10^3)	88 (65×10^3)	241 (177×10^3)	.89

[a]Rate until zero power is achieved; under rotor speed control at a slower pitch rate until 20 rpm is reached; rate then returns to 0.8°/sec until full feather.

TABLE IV. - COMPARISON OF CYCLIC BLADE LOAD DATA FOR SEVERAL CONFIGURATIONS OF 200-kW MOD-0A WIND TURBINE

Test configuration		Test period, revolutions	Mean wind speed, m/s(mph)	Flatwise cyclic bending loads				Chordwise cyclic bending loads			
Location	Blade type			Reference load,[b] kN-m (lb-ft)	Ratio of cyclic load to reference load		Ratio of 99.9th to 50th percentile	Reference load,[c] kN/m (lb-ft)	Ratio of cyclic load to reference load		Ratio of 99.9th to 50th percentile
					50th percentile	99.9th percentile			50th percentile	99.9th percentile	
Clayton, NM	Fiberglass	162×10^3	8.5 (19.0)	139 (102×10^3)	0.24	0.85	3.5	54 (40×10^3)	1.03	1.35	1.31
Clayton, NM	Aluminum[a]	102×10^3	9.3 (20.8)	135 (99×10^3)	.22	.85	3.9	61 (45×10^3)	1.10	1.48	1.35
Kahuku, HA	Wood[a]	126×10^3	8.8 (19.7)	152 (112×10^3)	.24	.74	3.1	69 (51×10^3)	1.12	1.51	1.35

[a]Reference 6.
[b]Calculated aerodynamic bending moment change from zero to rated power.
[c]Measured gravity bending moment.

Figure 1. - 200-kW Mod-0A wind turbine with SCI fiberglass blades at Clayton, NM.

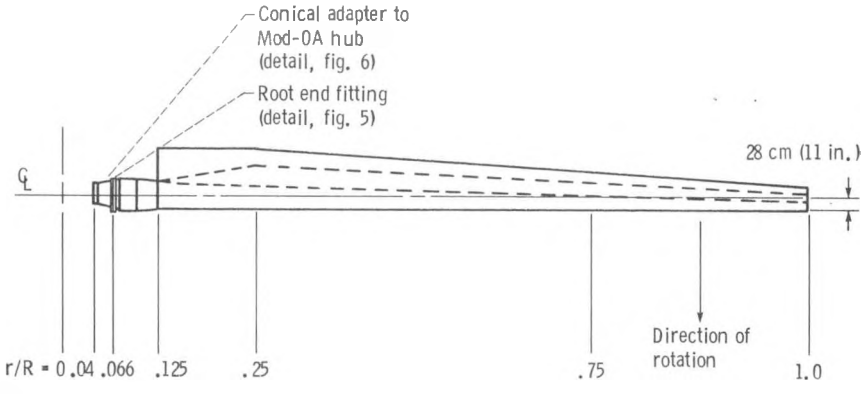

Airfoil (NACA series)	--	23030		23018	23012
Twist, deg	-8	-4		0	2
Chord, cm (in.)	140 (55)	140 (55)		84 (33)	56 (22)

Figure 2. - Definition of SCI fiberglass blade geometry (R = 19.06 m (62.5 ft)).

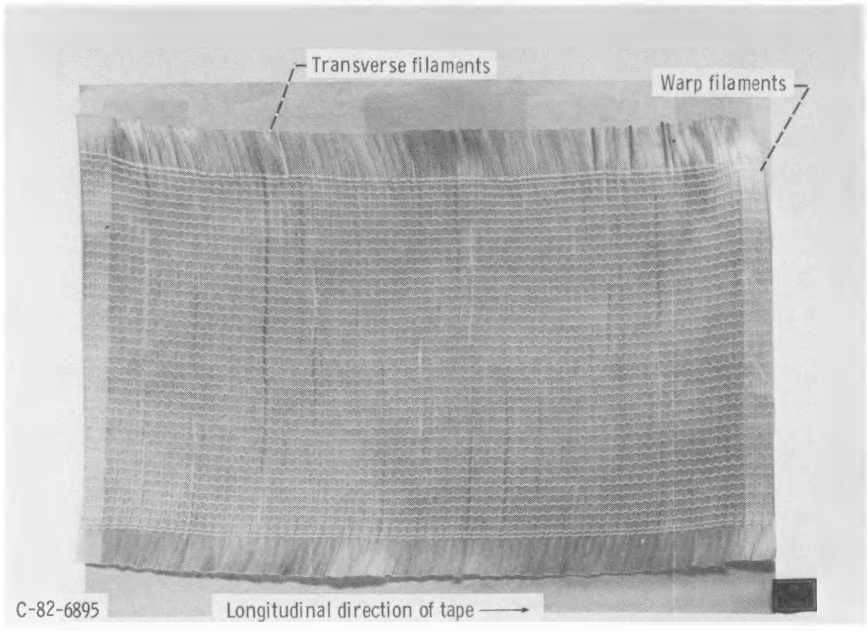

Figure 3. - Transverse filament tape (TFT).

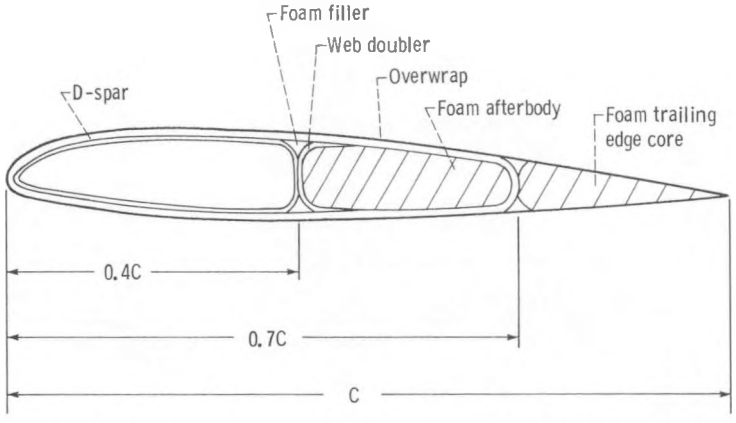

Figure 4. - Typical cross section for SCI fiberglass blade (NACA 230XX series).

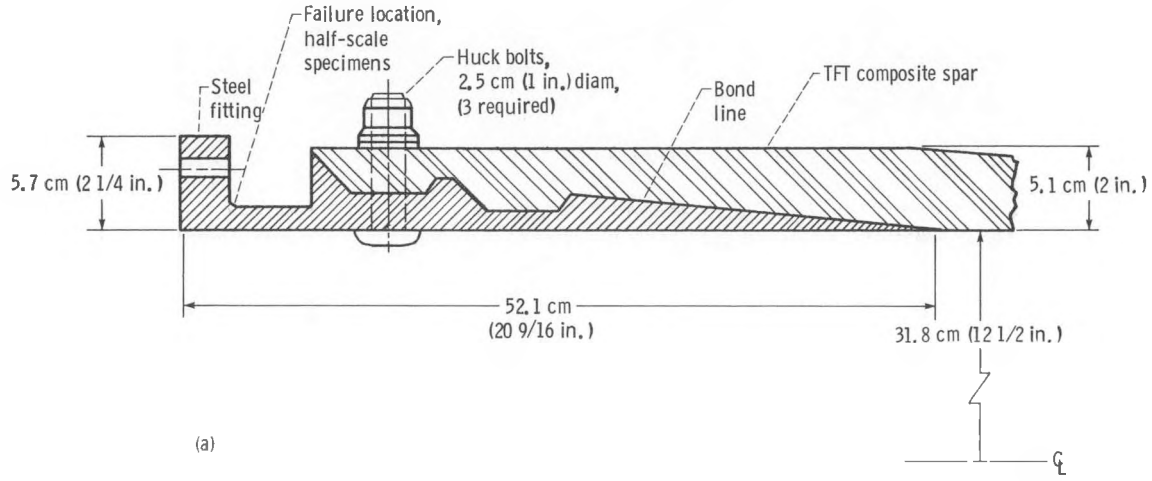

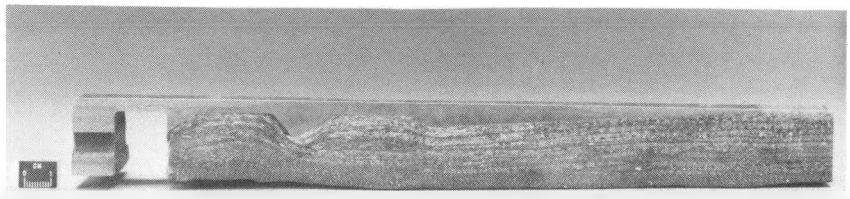

(b)

(a) Components and dimensions.
(b) Photograph of sectioned half-scale specimen.

Figure 5. - Root end details for SCI fiberglass blade.

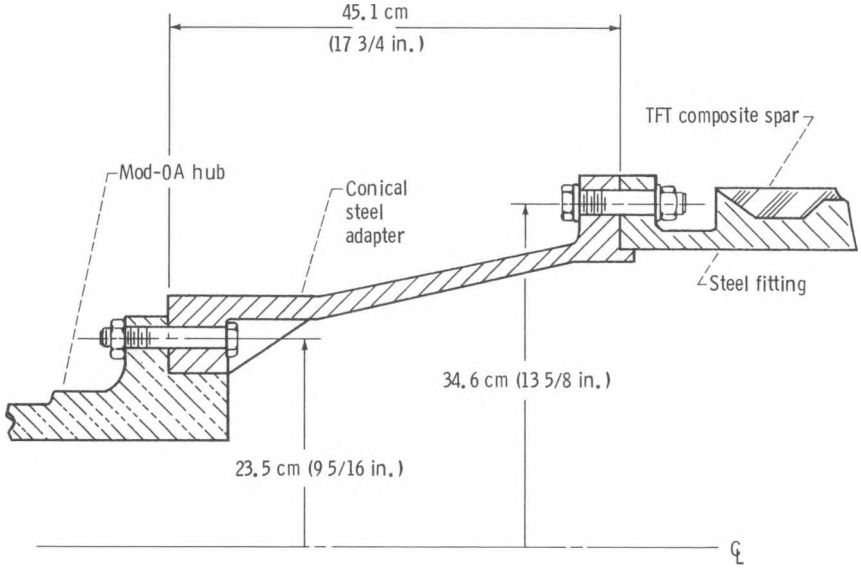

Figure 6. - Blade-to-hub adapter for SCI fiberglass blade.

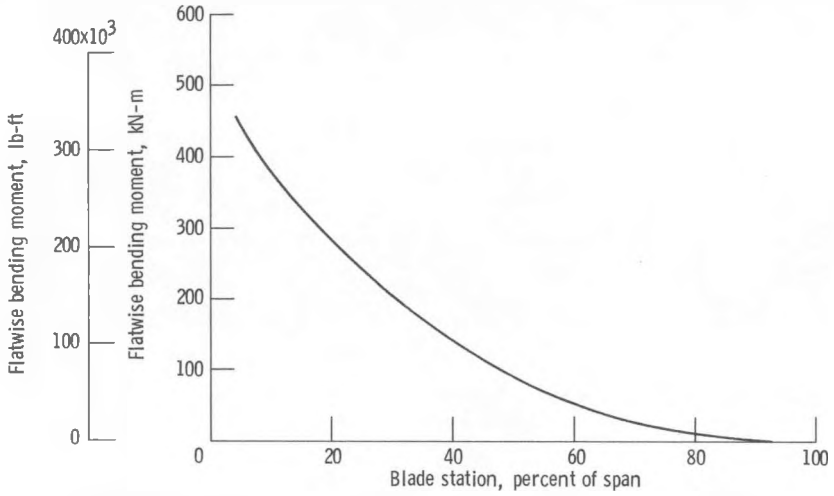

Figure 7. - Bending moment distribution for SCI fiberglass blade limit load design condition.

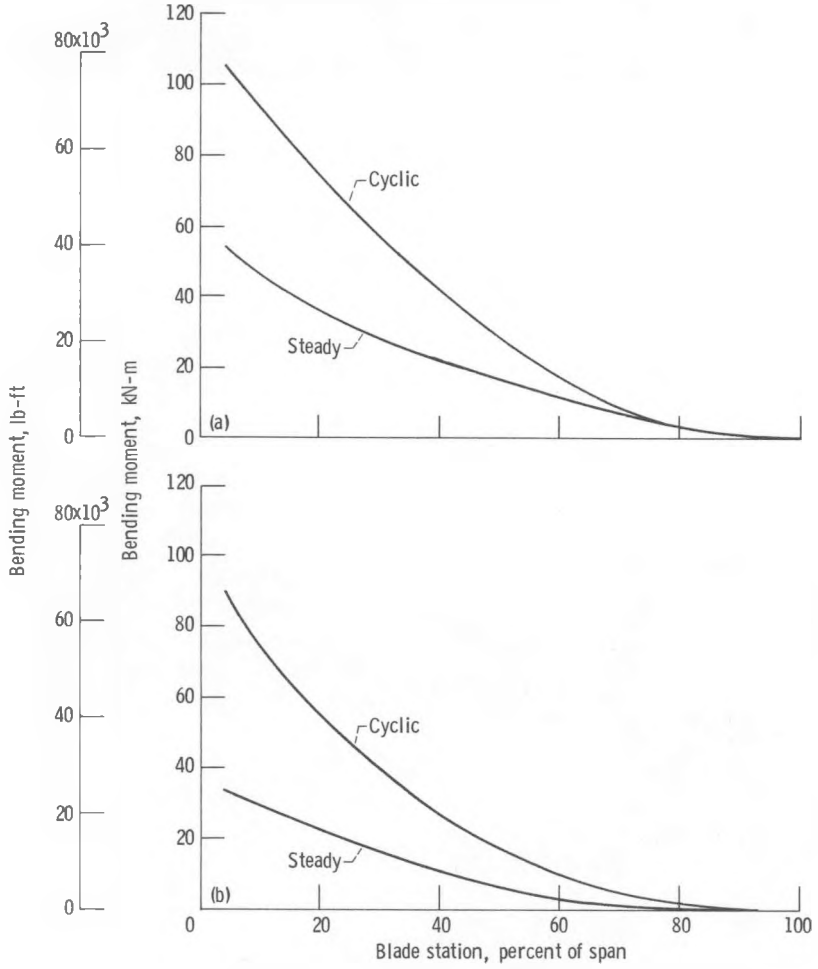

(a) Flatwise.
(b) Chordwise.

Figure 8. - Bending moment distribution for SCI fiberglass blade fatigue load design condition.

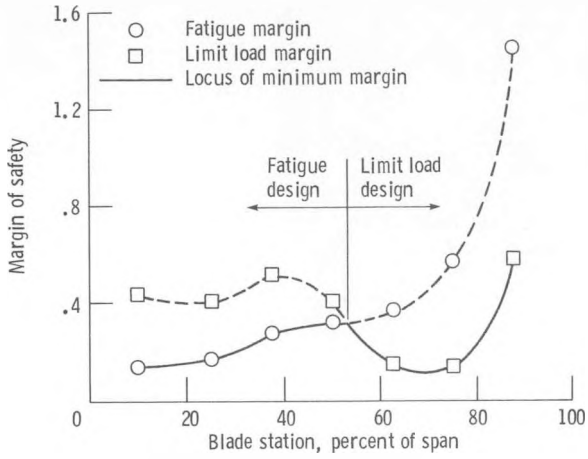

Figure 9. - Spanwise distribution of margin of safety for the SCI fiberglass blade design.

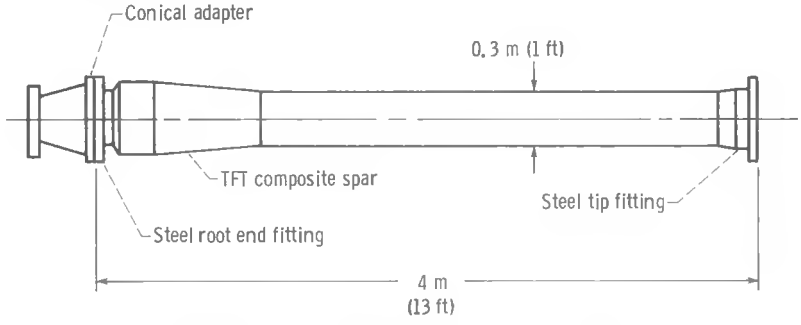

Figure 10. - Half-scale root end fatigue test specimen.

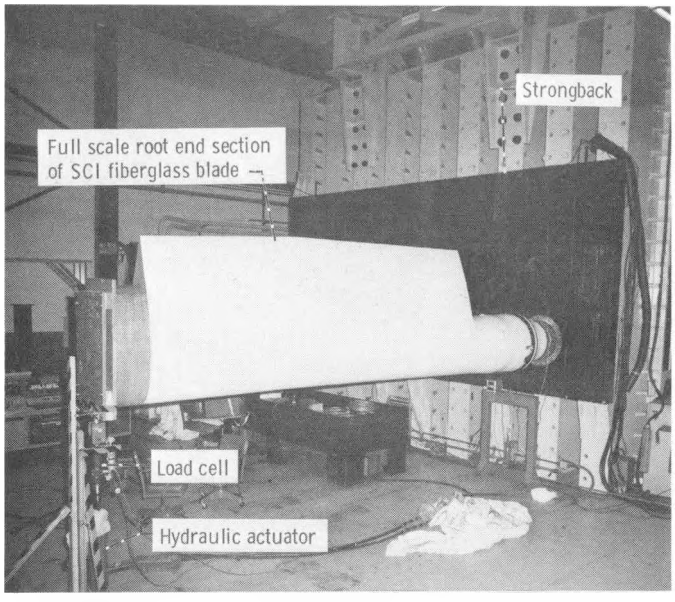

Figure 11. - Blade section in structural fatigue test facility at the NASA Johnson Space Center.

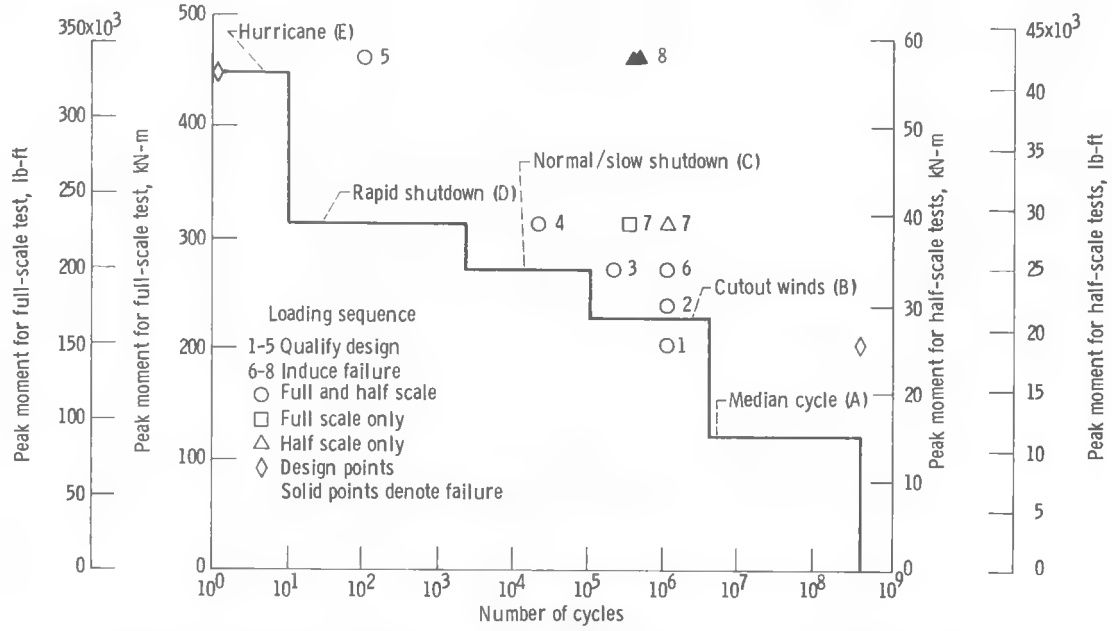

Figure 12. - Comparison of expected loading spectrum with qualifying spectrum for SCI fiberglass blades (5 percent span).

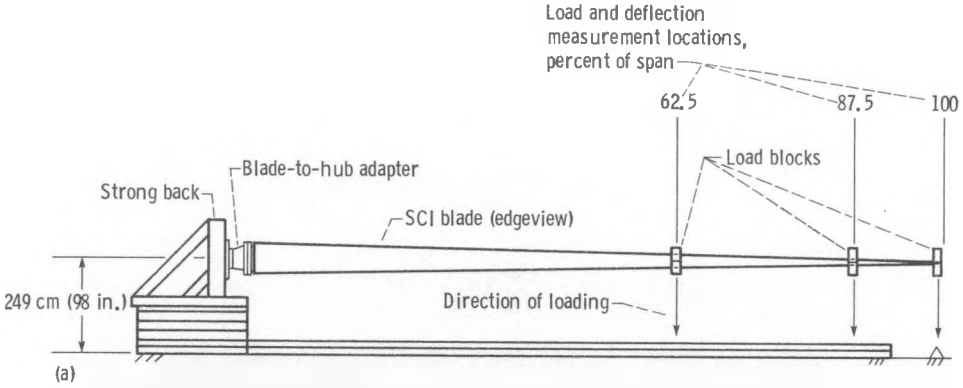

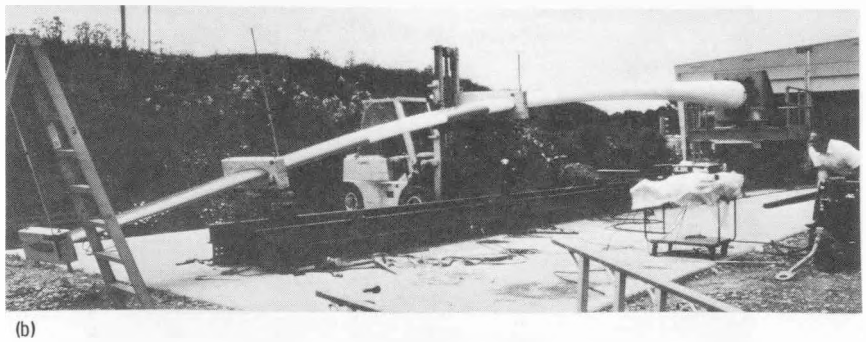

(a) General arrangement for blade test.
(b) Blade under load.

Figure 13. - SCI fiberglass blade in the NASA Lewis wind turbine blade static test facility.

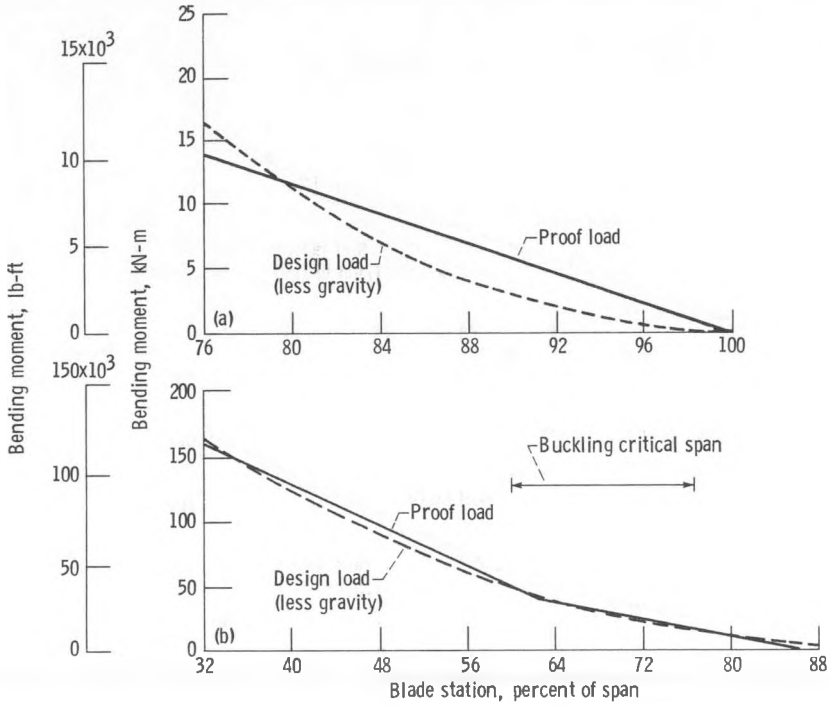

(a) Tip section.
(b) Midspan section.

Figure 14. - Comparison of applied proof load and design limit load for SCI fiberglass blades.

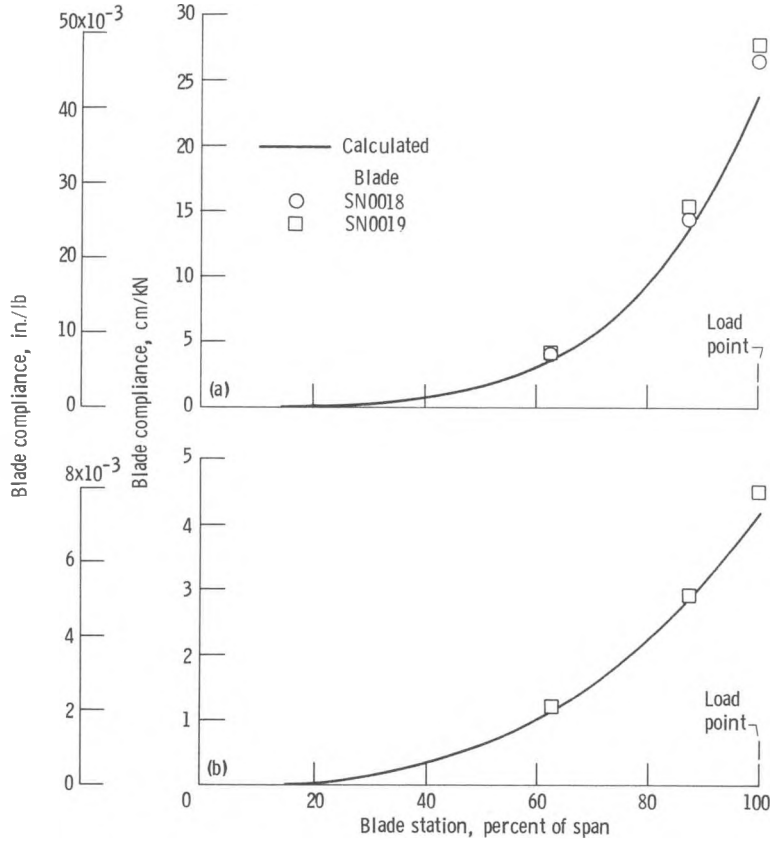

(a) Loaded perpendicular to chord.
(b) Loaded parallel to chord.

Figure 15. - Comparison of measured and calculated compliance of SCI fiberglass blades (rigid retention).

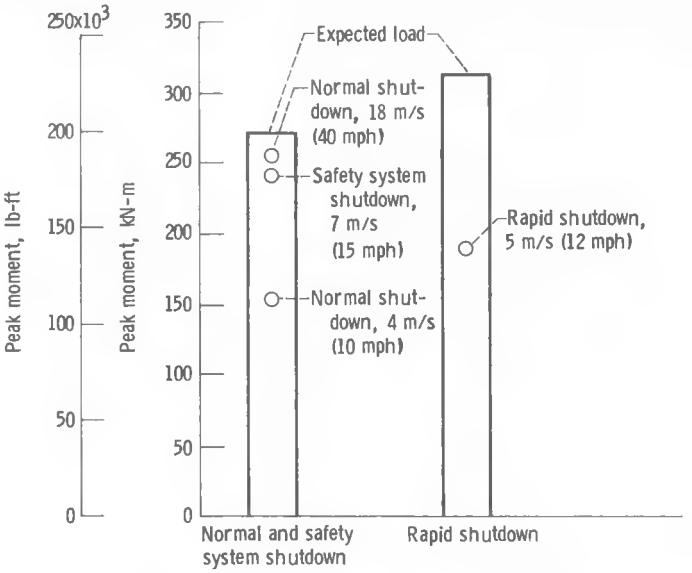

Figure 16. - Comparison of measured and expected loading during Mod-0A shutdown with SCI fiberglass blades (5 percent span).

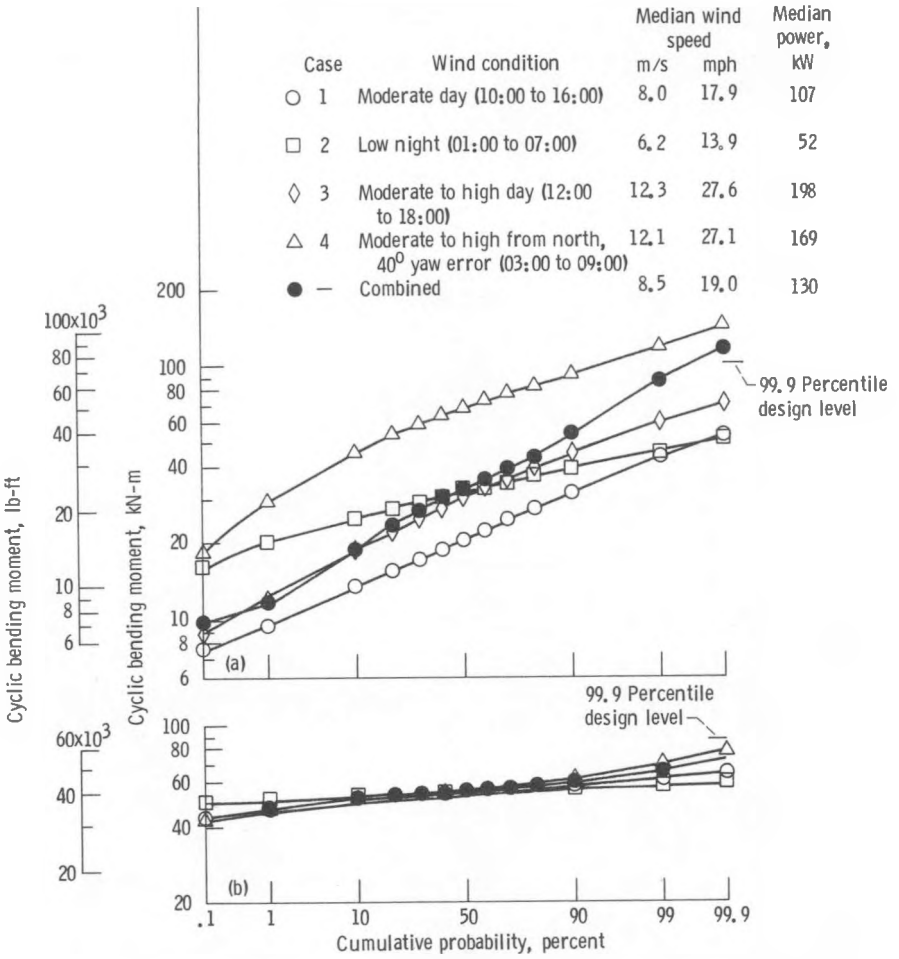

(a) Flatwise.
(b) Chordwise.

Figure 17. - Spectra of measured fatigue loading for SCI fiberglass blades on Mod-0A (5 percent span).

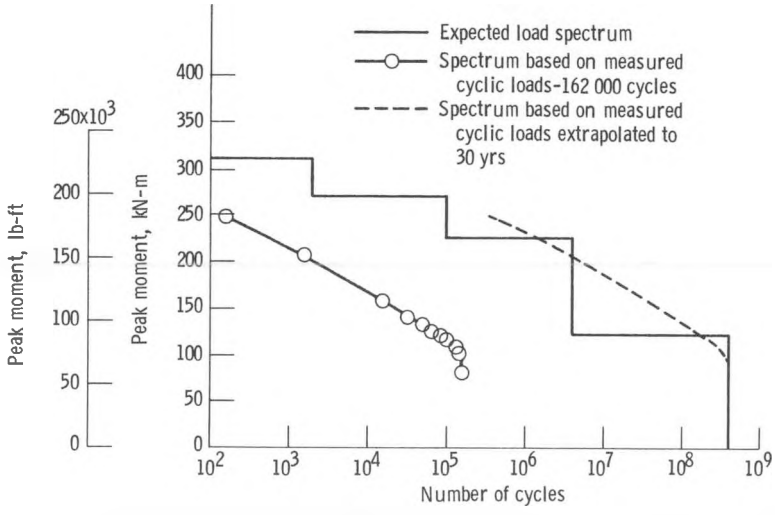

Figure 18. - Comparison of expected fatigue loading spectrum and spectrum based on measured cyclic loads for the SCI fiberglass blades on Mod-0A (5 percent span).